Second International Symposium on

WIND ENERGY SYSTEMS

October 3rd - 6th, 1978

PAPER B6

WAKE INTERACTION IN AN ARRAY OF WINDMILLS. THEORY AND PRELIMINARY RESULTS

T. Faxén

University of Uppsala, Sweden.

Summary

The paper describes a model developed by Lissaman (Refs. 1 and 2) for predicting power output of a general array of wind turbines. This involves a computer program capable of handling any number of identical wind turbine units at any power coefficient or height in an array of arbitrary geometry on level terrain, as the wind direction varies through 360°.

The fluid mechanics of wake development are analysed and it is shown that the momentum deficit behind each unit will be c onserved downstream. Thus, if radius and wake profile are known, the wake velocity can be determined. Wake profiles established from previous experimental work in co-flowing jets are used, and wake radius determined by assuming the wake growth is caused by both ambient and mechanically generated turbulence. The latter controls the initial growth, while ambient turbulence dominates the downstream development. A procedure to handle the combined effects of ambient and mechanical turbulence is given. Ground effect is simulated by imaging techniques, and multiple turbine interactions by averaging and superposition methods.

An example on the use of the model is presented. The results indicate that for large arrays significant power losses can occur for improper geometry.

The importance of natural turbulence is surveyed. This shows that the bigger the array, the more important it is to get an estimate of this turbulence.

Finally, wake profiles obtained in field tests at the 60 kW test unit at Kalkugnen, Sweden, are compared to what is predicted by the model. A very good correlation is found which strongly supports the model.

Held at the Royal Tropical Institute, Amsterdam, Netherlands.

Symposium organised by BHRA Fluid Engineering in conjunction with the Netherlands Energy Research Foundation ECN

Nomenclature

α — Rms turbulent velocity ratio q/U

ΔU — Velocity deficit between undisturbed flowspeed and wake velocity

ΔU_{mo} — Velocity deficit between undisturbed flowspeed and centerline wake velocity.

C_p — Power coefficient for a wind turbine

P — Effective power

P_i — Effective power for turbine no i

q_t — Effective rms ambient turbulence, $q_t^2 = u'^2 + W'^2 + V'^2$

r — Wake radius

R — Wake edge radius

σ — Plume width

u — Wake velocity

U_0 — Free stream velocity

U_{mo} — Wake velocity at the centerling

V_T — Total turbulent velocity, $V_T^2 = V_{TM}^2 + V_{TA}^2$.

V_{TM} — Turbulent velocity due to momentum effects

V_{TA} — Turbulent velocity due to ambient effects

X — Downstream distance

X_H — Potential core length

X_N — Distance to effectiv far wake profile

Introduction

The effectiveness of a Wind Energy Collection System (WECS) depends crucially on the available wind energy. For units positioned in an array, the energy extraction by downwind units is reduced. The amount of this energy degradation is of critical importance in assessing the system cost effectiveness.

Since the Swedish policy is to build large arrays in favorable locations it was decided by the National Board for Energy Soure Development (NE) that research was to be made in this area. One of the principal contributions here is the model which Dr Peter Lissaman at Aerovironment Inc. developed under contract to NE. During part of this period the author worked directly with Dr Lissaman. The work was performed in two phases during the period October 1976-May 1977 and resulted in two reports: Energy Effectiveness of Arrays of Wind Energy Collection Systems Phase I (Ref. 1) and Phase II (Ref. 2). At the end of the paper some model predictions are compared with measurements around a wind power test unit in Sweden.

General fluid physics

Because of the many variables that are involved in the wakeflow in a typical wind turbine array the prediction of interaction between multiple wakes becomes exceedingly complex. Furthermore work in this area is quite new so there is a lack of relevant test data. For these reasons we have to simplify the problem and look for parallels. We assume that the wake of a single power generating rotor to be quite similar fluid mechanically to that of a circular jet immersed in a uniform flow, as shown by Abramovich (Ref. 3). The word jet is usually associated with a flow of higher speed than the outer flow but in all cases here the speed is lower than that of the outer flow. That is the jet is actually wake- like, a case also extensively studied theoretically and experimentally by Abramovich. The general process of wake development behind the turbine is that the wake grows by turbulent entrainment at its edge which introduces free stream momentum as well as mass into the wake while conserving certain global properties.

There are three controlling parameters for the wake development:

a) For a constant pressure wake the momentum deficit in the wake is conserved. This describes the turbine drag and must be constant downstream. This is defined by the integral $\int \frac{u}{U_0}(1-\frac{u}{U_0})r\,dr$ across the wake

b) The wake growth rate $\frac{dR}{dX}$, defined by the turbulent mixing.

c) The wake profile at given radius r given by $\frac{u}{U_0}=F(\frac{r}{R})$, defined by various similarity profiles with experimentally determined constants.

To simplify the analysis we assume a uniform incoming wind profile and uniform incoming natural sheargenerated turbulence.

The momentum deficit in a) can be computed from the initial profile of the wake which can be directly related to the drag of the rotor and the power output.

Abramovich defines the nondimensional profiles of the wake using analytical forms of the velocity profiles, based on a large amount of experimental data from turbulent jets. These profiles varying in a downstream direction, progressing smoothly from the initial profile immediately downstream of the rotor to the asymptotic profile far downwind. This gives us c).

For a nonturbulent outer flow mechanically produced turbulence is developed by the velocity gradient at the wake edge and by the rotor itself (rotational terms which are small and neglected). In a nonturbulent outer flow this turbulence completely controls the rate of growth of the wake.

However when the rotor is immersed in an outer flow containing ambient turbulence this turbulence will in some way add to the mechanically produced turbulence present. The mechanically produced turbulence which is related to the wake radius and velocity deficit rapidly decays, so that the wake growth rate due to this effect steadily decreases. We then expect that the ambient turbulence will start to control the wake growth as the rotor and momentum turbulence decays.

We now assume that the two turbulence generation processes occur independently as seems likely because of the large differences in scales of the generative processes, and that the two turbulent energies are thus additive. We can then write

$$V_T^2 = V_{TM}^2 + V_{TA}^2$$

where V_T is the total effective turbulent velocity near the wake edge and V_{TM}, V_{TA} that due to momentum and ambient effects respectively.

Assuming that the wake growth at the edge of the wake is proportional to the total effective rms turbulent velocity in that region, regardless of how this turbulence has been generated we get the wake growth $dR/dX \simeq V_T/U$ yielding

$$(dR/dX)^2 = (dR/dX)_M^2 + (dR/dX)_A^2$$

Abramovich gives us $(dR/dX)_M$ as a function of the difference between the undisturbed flow speed and the centerline velocity $(dR/dX)_M = F(\Delta U_{mo}/U_o)$

To get an estimate of $(dR/dX)_A$ we study the growth of the plume of an entirely passive contaminant, that is one containing no relative momentum, like a pollution dispersion. It can be shown for short range dispersion according to Taylors theorem that the plume dimension σ grows approximately proportionately to the ambient turbulence, $d\sigma/dX \sim \alpha$, where α = rms turbulent velocity ratio σ_T/U. We can now equate the scalar transport of the Gaussian distribution used in plume analysis to the particular near Gaussian distribution used for the velocity deficit. This gives us $dR/dX = \alpha/0.51$ where the numerical constant 0.51 connects the outer wake radius of the Abramovich profile with the effective plume width.

The constant α can be calculated from the environmental conditions of wind speed, ground roughness and insolation which control the wind ambient turbulence.

We then assume that the natural windshear turbulence generating process is sufficiently strong that changes within the array can be neglected which gives us a constant α within the array. We can now evaluate the last controlling parameter c). Figure I shows the geometry of the wake as given by Abramovich but modified for a turbulent outer flow. The wake is divided into four regions. In the first region a turbulent region extends outward and inward from the edge of the wake surrounding the potential core of uniform flow. The initial region terminates when these shear layers meet at the center so that the center velocity deficit starts to reduce. As it progresses downstream the wake profile transitions from this profile to the asymptotic far downstream profile.

The analytical expression for the velocity profile changes from the end of region I to region III so region II becomes a transition region. In region III and IV we have new selfsimilar asymptotic profiles. Figure 2 shows the different velocity profiles in the four regions drawn to the same scales for both radius and centerline velocity decrement respectively. It should be noted that in a given situation the far wake profile will have a large radius and small velocity deficit. In region I and II calculations show that the ambient and momentum turbulence are of the same magnitude, while in region III the momentum turbulence decays and in region IV it can be neglected and the flow is dominated by ambient turbulence.

The geometry of the wake is now a function of α and the power coefficient C_P for the turbine. Changing α and C_P results in a stretching or shrinking of region I and II, region III is set as 10x radii, numerical calculations having shown that mechanical turbulence has always decayed in this length. Table 1 shows some examples of this.

For given α and C_P, the equations for the velocity profiles now give us the velocity decrement anywhere in the wake. This velocity decrement will be calculated as a multiple of the free stream speed $\Delta U = k \cdot U_o, k<1$.

Effect of neighboring wakes

In an array of turbines we will get a complex field of overlapping and interacting wakes. In the case of two overlapping wakes the momentum generated turbulence will be affected by the interaction of the two wakes. However, as mentioned in an earlier section, the momentum generated turbulence is negligible compared to the ambient terms after a few tens of radii downstream. Thus the transfer of velocity deficit will be similar to that of an inert scalar. The situation then becomes analogous to pollution concentration due to neighboring plumes. Where, because of the linearity of the process one may simply superimpose the respective plume concentrations. This superposition conserves pollutant mass in the analog situation and in our case conserves the momentum deficit, or drag of each unit, and thus satisfies drag conservation.

For the case where a turbine is immersed wholly or partly by a wake, this reduces the mean velocity over the turbine disc. This reduced mean velocity is calculated and used as the new incoming velocity for that turbine. Furtheron we assume that the turbulence created by this turbine does not affect the growth of the impinging wake further downstream.

The situation is sketched in figure 3 where we can see that all the wakes are simply superimposed. This super imposition means that to find the velocity we simply add the velocity decrements from the wakes involved and subtract this from the free stream velocity.

Ground effect

The ground plane has an effect in reducing vertical downward wake growth both by the suppression of turbulent velocity near the ground and by the direct presence of the ground (the image effect). For the concentration of inert pollutants the ground effect has been extensively studied and the standard approach is to model it by classical reflexion techniques. In the case with wind turbines this means that we place an image turbine at a distance below the ground plane equal to the height above the ground of the actual machine. This produces two parallel offset and eventually overlapping wakes oriented vertically as shown in figure 4. The velocity decrement from the two wakes is added in the manner described previously for the overlapping of conventional wakes. This model does not directly account for the suppression of turbulence near the ground but gives rational ground effect profiles, conserves momentum deficit and assure no wake momentum transfer into the ground.

Power calculation

Since we now have the velocity decrement anywhere in the array we can compute the mean velocity over each turbine disc as a multiple of the free stream velocity.

$$\bar{U}_i = k_i \cdot U_0, \quad k \leq 1.$$

Cubing this we get the power available for each turbine as a multiple of the free stream power

$$P_i = k_i^3 \cdot P$$

This can be done for an arbitrary array and, with the help of a coordinate system that rotates with the incoming wind, for an arbitrary wind direction.

Computer code

Routines for the calculations described in previous sections were written assuming.

a) Flat and level terrain
b) uniform incoming windprofile.

This is an approximation to the actual situation, where the planetary boundary layer produces a vertical shear gradient. The present model assumes that the wind speed at the turbine axis will be a satisfactory approximation for the non-uniform wind field.

c) All the turbines operate at a constant power coefficient C_p

d) The tower shadow is neglected.

The computer model now gives us the effective mean power ratio:

$$(1/n) \sum_{i=1}^{n} (k_i)^3 \quad , \; n = \text{number of windmills}$$

from an arbitrary array with arbitrary oncoming wind-direction. This ratio is the ratio of the array power to the array power for each turbine operating in a free stream. The effective power ratio $(k_i)^3$ for each turbine is ofcourse also available.

The inputs to the computer code are, besides the windmill coordinates and wind-direction, the ambient turbulence α, power coefficient C_p and height above the ground of the turbine. The model is valid for both horizontal and vertical axis machines. The magnitude of the oncoming wind is not needed since the model always works with the ratio between the free stream velocity and the wake velocity and the ratio between the extractable power and the free stream power. This non-dimensional power ratio has to be multiplied with the free stream power to get the magnitude of the extractable power for each wind turbine. However, the magnitude of the wind may affect the ambient turbulence term α.

Further refinements to the computer model, for example, boundary layer flow, non level terrain and operation of the individual wind turbines at variable C_p will produce changes in the model output. However the primary form of the relationship between array power and wind direction is determined by the array geometry and the manner in which the wind turbine wakes interact with each other and with other wind turbines in the array. This is all accounted for in the present model and as such the model represents a very valuable tool for the engineering design of wind turbine arrays.

Exercise of computer model

As the computer model stands today it is simple and efficient to use for investigations of various array geometries. This has been done for a number of cases from the simplest case with only two windmills up to complex configurations of 80 units in irregular arrangements. To illustrate this and how the model can be used in a future planning of WECS we first take a look at a study performed by the Swedish State Power Board published in a report from NE (Ref. 4).

The intention was to simulate a case with planning of an array to get an idea of the work that is to be done in a real case. To do this a number of sites with strong winds and flat levelled terrain were selected. When doing this, concern was taken to housing, nature reserve and areas for open air life. For each site an array of turbines was simulated and in this detailed planning, roads, landscape, farming, power-lines etc. were taken into consideration. Depending on the size of the array the following minimum distance between two adjacent windmills were given, based on earlier results by Carl Crafford (Ref. 5): array ≥ 100 units minimum distance 20 radii, 25 ≤ array < 100 units minimum distance 14 radii.

The size of the turbines were 25 or 50 meter radii (1 or 4 MW), hubheight 50 or 100 meters. Figure 5 shows one of the sites in northern Uppland where a large array of 80 windmills was arranged in two rows across the prevailing winddirection. The great power and engineering value of the Lissaman model is that a truly arbitrary array can be selected. We do not have to confine arrays to square grids, hexagons or the like, but are free to define any array in a real world, accounting for any topographic or man made features. This makes it of immediate practical value for WECS planners.

We now apply the Lissaman model on this study. To do so we first input the coordinates for each windmill which we simply get by placing a coordinate system on figure 5, see figure 6. Assuming a power coefficient $C_p = 0.5$ and ambient turbulence $\alpha = 0.05$, which is representative for a case with moderate winds (> 2 m/s) blowing over flat grassland (z_0=0.10 m) in a neutrally stratified atmosphere, we get the values illustrated in figure 7.

This shows that the model predicts an even energy production except for the case when the wind blows along the array axis, i.e. from 120° and from 300°. The mean power ratio $\bar{P}$ was calculated using the wind-direction distribution which is also in the figure. For each wind-direction class, the mean power ratio in that class was multiplied with the number of cases with wind from that direction, counted as a percentage. These classes were then added to get $\bar{P}$.

The Lissaman model also provides the power ratio of each individual unit. This information can be of value for further optimizing the exact siting of the wind turbines.

The great advantage with the present model is the freedom to change the windmill coordinates and the wind-direction. Coupled with appropriate data on α and C_p for a selected site this gives us the opportunity to calculate the energy production for any array and any wind-direction. Using the model in this way one has a great engineering and planning tool for finding the optimum design of an array of windturbines.

The ambient turbulence α

To get an understanding of the importance of α a number of cases were run with several α values in the range

$$0.0 < \alpha \leq 0.10$$

which represents cases from very stably strafied atmosphere with practically no turbulence to cases with strong winds in rough terrain.

The results so far indicate that for small arrays the turbulence term is not so important if we look at the mean power ratio for the whole array and all wind-directions. It seems that with low turbulence the wake is narrow and contains a large momentum deficit, but since the dimensions of the wake are so small it rarely hits the other windturbines in the array. When the turbulence is stronger the wake is wider and the velocity deficit diluted. This wake hits other turbines more often but with weaker strength. In the average this means that the difference between high and low turbulence cases is small as long as the size of the array is small.

For an array of 4 units, with the windmills placed in the corners of a square with the side 4 radii, the difference in mean power between $\alpha= 0.01$ and $\alpha= 0.10$ is only 2-3 percent. When the array grows this difference also grows. For the case in figure 7 cited above the following results were found

$\alpha= 0.0$	$\bar{P}= 0.751$
$\alpha= 0.05$	$\bar{P}= 0.837$
$\alpha= 0.10$	$\bar{P}= 0.883$

We see that there is up to 13% difference. When the array grows in size the wakes in the turbulent case soon becomes so diluted that they do not affect other turbines while for the nonturbulent case they still hold a large amount of velocity deficit at great distances. This supports our intuition that in strong ambient turbulence there cannot be persistent wake effects. This implies that the bigger the array the more careful one should be in getting a good estimate of the expected turbulence at the site. The implication being that a large array, with many straight lines of units, can experience severe 'flat spots' in power when wind with weak turbulence blows parallel to a line of turbines.

Wake measurements

At the 60 kW test unit in Kalkugnen,Sweden, continuous measurements of windspeed, winddirection, temperature and effective power have been made since September 1977. (ref. 6). Two 42 m high masts are equipped with cup anemometers at 6 levels and wind-direction vanes at two levels. Temperature is measured at 6 levels in one of the masts but this instrumentation is not functioning fully yet. Fig. 8 shows a map of the site and the location of the masts and the windmill. One of the purposes with the meteorological program was to investigate the wake of the windmill. This was also the main reason for placing the masts and the test unit on a straight line. During the period October to December 1977 a case of 4 hours duration occurred when the turbine extracted energy from the wind and the direction of the wind was along this line.

Fig. 9 shows one of the 1 min mean wind profiles. The winddirection was between 20-40 degrees. In order to get an estimate of the wind velocity deficit in the wake one must compare profiles from the same mast. This is so because with winds from this sector, the two masts experience wind from different downwind fetches. The north mast experiences both a sea and a land fetch but the south only a land fetch (which is partly the same as that for the north mast). They therefore exhibit different wind profiles and cases with and without energyextraction must therefore be evaluated from the same mast. The undisturbed profiles from the other mast can then be used as a check that the wind is blowing from this sector and that the meteorological conditions were similar. To be able to calculate the velocity deficit we must therefore in some way reconstruct the original undisturbed profile. Fig. 10 shows the mean wind profiles for the sector 20-40° in October and November 1977. We clearly see that the profile for the south mast can be approximated with two straight lines. Since we can expect near neutral conditions this is consistent with the logaritmic windlaw. The two straight lines can be identified as two boundary layers one from the open rough country between the seashore and close to the mast and one from the clearing around the mast. For the north mast we get the same picture but we there also find a boundary layer related to the sea in the upper three levels. When the wind is coming from this sector it faces very similar open rough country for the two masts. This means that the boundary layers from this open rough country, seen in level 2-6 in the south and level 2-3 in the north mast, are the same. This is verified from a number of cases without energy extraction and can also be seen in figure 10. We can now find the slope for level 2-6 in the south mast with the help of data from the north mast.

In a case with energy extraction we now assume that the velocity deficit at the 7 m level can be neglected. We can then start the reconstruction of the undisturbed wind-profile from there. From a number of windprofiles without energy extraction it is found that if we in a plotted windprofile like the one in figure 10 draw a vertical line from the 7 m level velocity we will cross the extended slope from level 2-6 at a fairly constant height between 10-12 m. (Dotted lines in figure 10). Roughly 30 percent of the profiles in the north mast from the case in October 1977 are undisturbed. From this material we can decide the height of this crossing point valid for that specific case. This was done and it was found to lie fairly constant at 10.5 m. Assuming this value to be valid for the rest of the profiles we can now reconstruct the undisturbed profiles for cases with energy extraction. In this way we find 12 clearly distinguished wake profiles. (The profiles are measured as the mean over one minute each tenthminute). Figure 12 shows the velocity deficit profile for two of those. In all the wake profiles the maximum velocity deficit is found at 27 m while the hub-height relative to the mast is 25 m. The landscape rises 5 m from the seashore to the windmill and then levels out. This is probably the reason for the difference between wake center and hub height. The question now is where in the wake the measured profile lies. The winddirection is not measured with accuracy enough to give the information we need. If we assume that all the 12 profiles lie in the center of the wake can we calculate what C_p that would give and compare this with the actual C_p measured by SAAB-Scania. C_p is found from the velocity deficit as

$$C_p = 1/2+(m^2-1-m)/2\ m^3$$

where m is defined as the ratio of the free stream velocity U_o, to that of the velocity in the wake immediately behind the turbine U_{mo}, $m= U_o/U_{mo}$. The results from this calculation is found in table 2 a). We see that there is a very good agreement for the first 8 profiles which implies that these profiles lies close to the centerline in the wake. The next four profiles have a lower C_p than needed which implies that these profiles are to be found in the outer region of the wake. The last profile has a higher C_p than possible. This can be explained as a result of the simplified method of reconstructing the profiles.

Column 1 of table 2 b) gives the energy deficit calculated from the first 8 profiles The second column gives the turbine power, for the calculated velocity deficit, calculated by SAAB-Scania. The good agreement gives further evidence to believe that these eight profiles lies close to the wake centerline.

For $z_o \simeq 0.4$ m, neutrally stratified atmosphere and winds in the range 6-10 m/s gives an $\alpha \simeq 0.10$.

It is now possible to make comparisons with the Lissaman model. Due to the limited amount of data we restrict this comparison to the wake radius. If the model is run for $\alpha \simeq 0.10$ and C_p is taken from column 1, table 2 a) we get the results in column 3 table 2 b). In column 4 are listed the radii obtained from the measured profiles. The agreement is excellent. In figure 12 is also indicated the shape of the velocity deficit profiles as predicted by the model (dotted lines). The agreement is very good but much more data is needed before any conclusions can be made. In the future we hope to get cases with varying ambient turbulence which would enable us to get profiles from various regions of the wake and thus check the predicted effects on the geometry of the wake as described earlier. However, the results so far indicate an excellent agreement between values predicted by the model and measured in field.

Conclusions

The important conclusions which can be drawn from this research are

1) The Lissaman model has a theoretical background which, although simply, correctly

and rationally incorporates all the major variables effecting WECS wakes.

2) The computer model requires only simple physical inputs, and can readily accomodate a completely arbitrary WECS array for all wind directions. The output gives the power available to each unit and the array as a whole. Changes in the array geometry or other inputs are easy to make and a profitable communication between the user and the model can soon be established. Thus it consitutes an important and useful engineering tool.

3) Exercise of the model has indicated that for large arrays significant power losses can occur for improper geometry.

4) Field experiments conducted by the Department of Meteorology, Uppsala University on the 60 kW WECS-unit at Kalkugnen, Sweden have strongly supported the model. Available data shows very good correlation with the Lissaman model.

Future work

The present model deals with the major aspects of the problem and forms a valuable frame work for investigating the effects of array geometry for many purposes related to technical and economic effectiveness of wind turbine arrays.

There are, however, three obvious areas in which future work could be profitably conducted. These are:

1) Testing of model against actual results obtained in field and windtunnel experiments. The field test is going at present.

2) Improving the meteorology and fluid mechanics incorporated in the model. This could be done by adding a meteorological boundary layer model which calculates the appropiate wind and turbulence profiles and by adding a more complex representation of the flow field as boundary layer flow.

3) Improving and augmenting the computer code by incorporating additional subroutines and refinements like a variable power coefficient C_p.

Acknowledgements

The author is happy to express his acknowledgment of the major contributions and valuable comments to this paper by Dr P.B.S. Lissaman who shared with him some of his deep knowledge of aerodynamics, meteorology and wind turbine technolcgy, as well as his friendship, during the author's stay at AeroVironment Inc. (California) in the spring of 1977. He would also like to express his appreciation of the excellent judgment of Sven Hugosson, program manager of NE and Dr Ulf Högström at the Department of Meteorology at the University of Uppsala.

Mr Hugosson made it possible for the author to visit AeroVironment, to use their excellent computer and instrumentation equipment and to collaborate with their outstanding scientists and technicians. Dr Högström's deep knowledge in meteorology especially turbulence and air pollution has been of invaluable help in evaluating the data and writing this paper.

The author acknowledges in this paper the warm relationships and excellent technical communication between Swedish and US researchers, and hopes it can extend to Wind Energy programs through out the world. Finally I also want to thank Mrs Maj-Britt Johannesson for typing the manuscript and Mrs Aina Ekström and Mrs Ulla Lindqvist for the drawing of all the figures.

References

1. Lissaman, P.B.S: "Energy effectiveness of arrays of wind energy collection systems, phase I". Aero Vironment Inc. Report AV R 6110. (January, 1977).

2. Lissaman, P.B.S and Bate, E.R: "Energy effectiveness of arrays of wind energy collection systems, phase II". Aero Vironment Inc. Report AV FR 7058. (May, 1977).

3. Abramovich, G.N: "The theory of turbulent jets". MIT Press. (1963).

4. National Board for Energy Source Development: "Windenergy in Sweden". (Vindenergi i Sverige, Resultatrapport juni 1977). Report NE 1977:2. (June 1977).

5. Crafoord, C: "An estimate of the inter action of a limited array of windmills". Department of Meteorology, University of Stockholm. Report DM-16. (November, 1975).

6. Faxén, T., Smedman-Högström, A.S and Högström, U: "The meteorological field project at the wind energy test site Kalkugnen, Sweden". Department of Meteorology, University of Uppsala. Reports No 51. (1978).

C_p \ α	0.01		0.05		0.10	
	X_1	X_N	X_H	X_N	X_H	X_N
0.463	27.6	40.4	10.7	15.7	5.6	8.2
0.563	18.4	27.6	10.5	15.7	5.9	8.9
0.588	14.7	23.0	10.1	15.7	6.2	9.6

Table 1. Values of potential core length X_H, and distance to effective far wake profile X_N, defined in figure 1, for varying ambient turbulence α and power coefficient C_p. All values are given in rotor radii.

N	$\bar{u}$	ΔU_m	C_{pc}	C_{pt}
1	8.2	2.1	0.39	0.39
2	8.0	2.0	0.39	0.39
3	8.6	2.7	0.39	0.43
4	8.0	2.0	0.39	0.37
5	7.3	1.6	0.39	0.35
6	7.7	1.6	0.39	0.35
7	11.1	2.4	0.31	0.33
8	6.0	1.0	0.33	0.28
9	7.5	1.0	0.39	0.23
10	6.2	0.7	0.33	0.17
11	6.9	0.8	0.36	0.20
12	9.8	3.2	0.35	0.46

Table 2a. $\bar{u}$ = Mean calculated undisturbed velocity over the rotor (m/s)
Δu_m = Velocity deficit at wake center (m/s)
C_{pc} = Calculated power coefficient from the profiles
C_{pt} = Predicted theoretical power coefficient

N	P_c	P_m	R_c	R_t
1	29	28	18	19
2	24	26	18	19
3	54	32	20	19
4	40	26	20	19
5	26	23	20	19
6	23	24	18	19
7	81	70	20	19
8	6	10	17	19

Table 2b. P_c = Power deficit calculated from the velocity deficit profiles (kW).
P_m = Measured power production at same wind speed as for P_c (kW).
R_c = Wake radius found from the velocity deficit profiles (m).
R_t = Wake radius calculated by the Lissaman model (m).

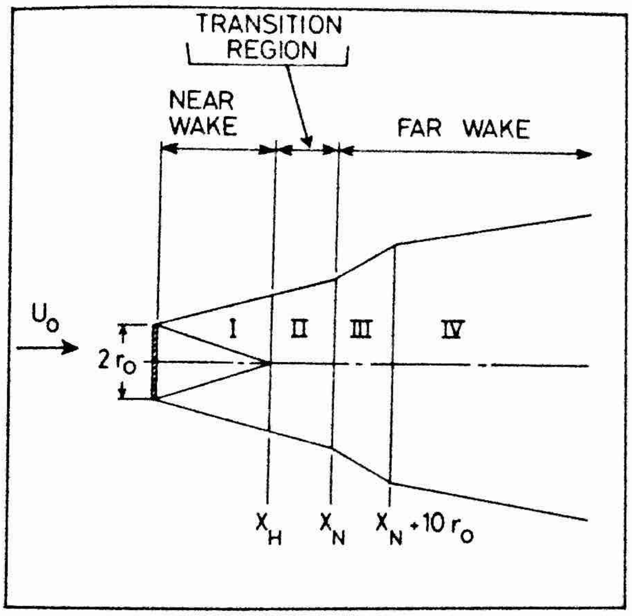

Fig. 1 Wake geometry as given by Abramovich but modified for a turbulent outer flow

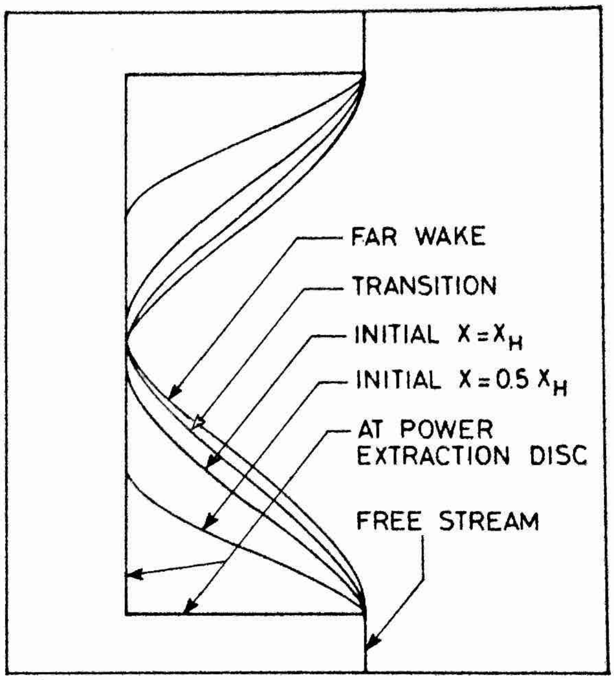

Fig. 2 Velocity profiles in the various wake regions

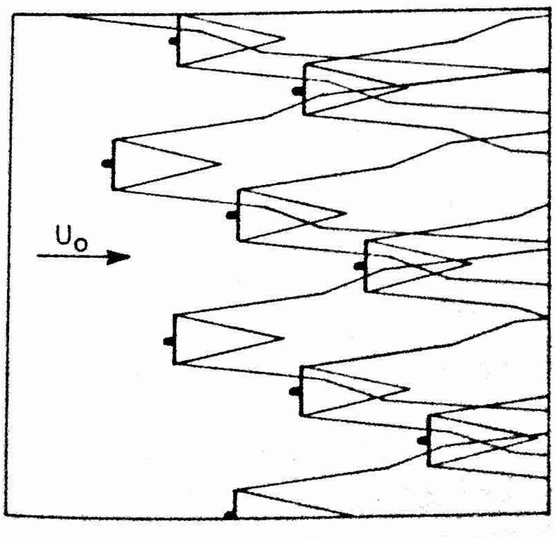

Fig. 3 Illustrates how the wakes in a wind turbine array are simply superimposed

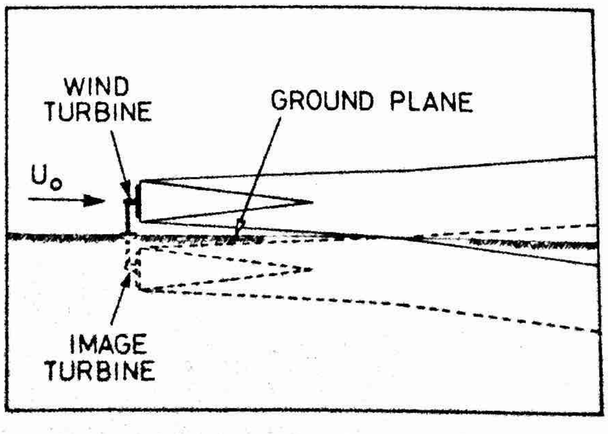

Fig. 4 Image representation of ground plane

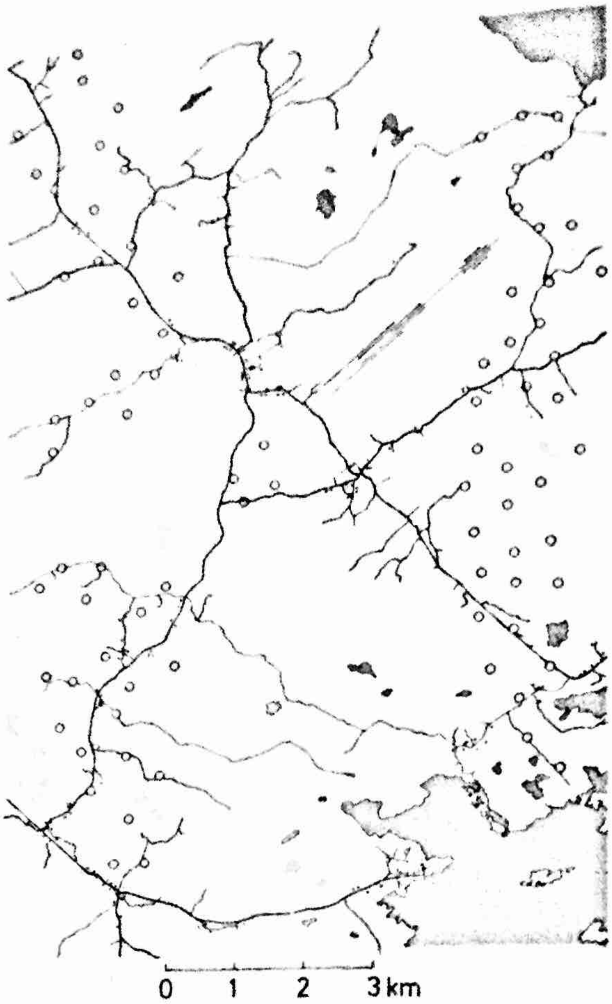

Fig. 5 Map of one of the real world theoretically planned test sites, with an array of 80 units.

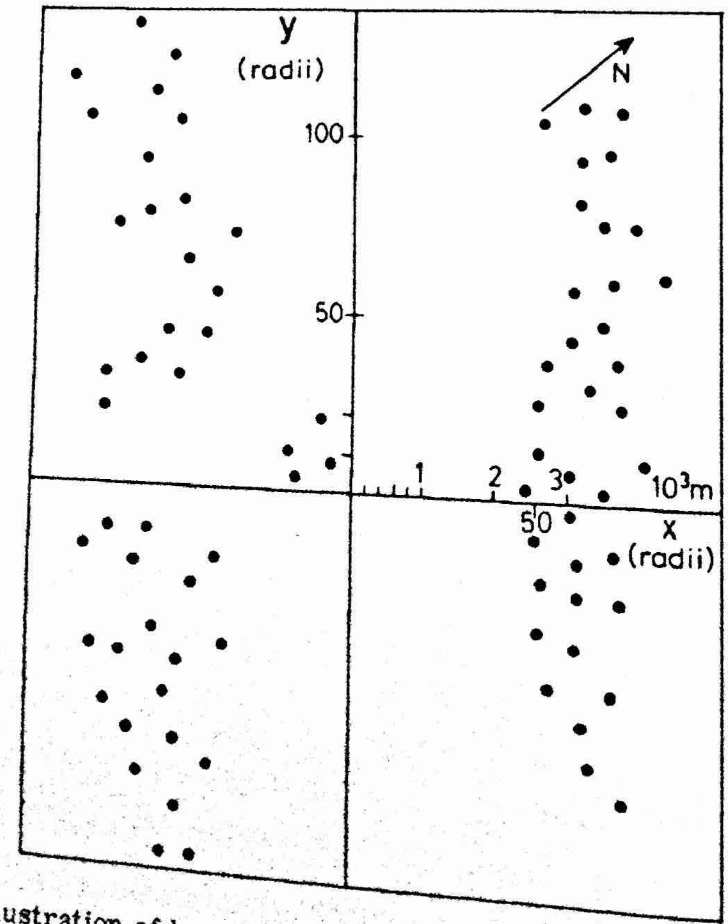

Fig. 6 Illustration of how to get the windmill coordinates from figure 5

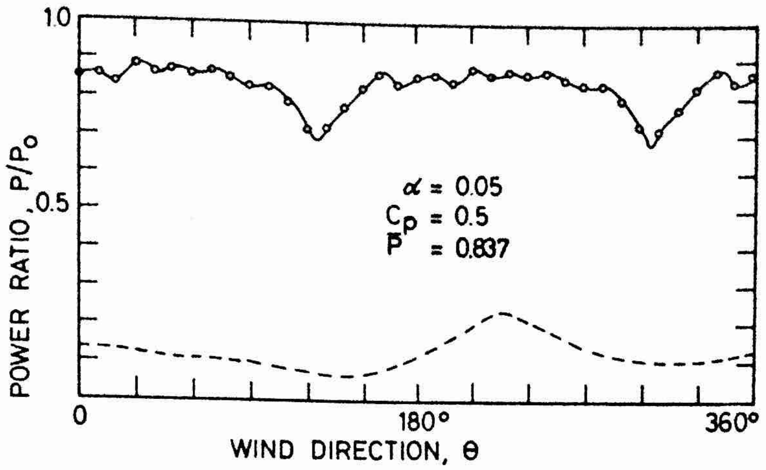

Fig. 7 Power ratio for the 80 wind turbine array in figure 5 as a function of wind direction. Also in the figure is the wind direction distribution counted as percentage where 1.0 equals 100% (dotted line)

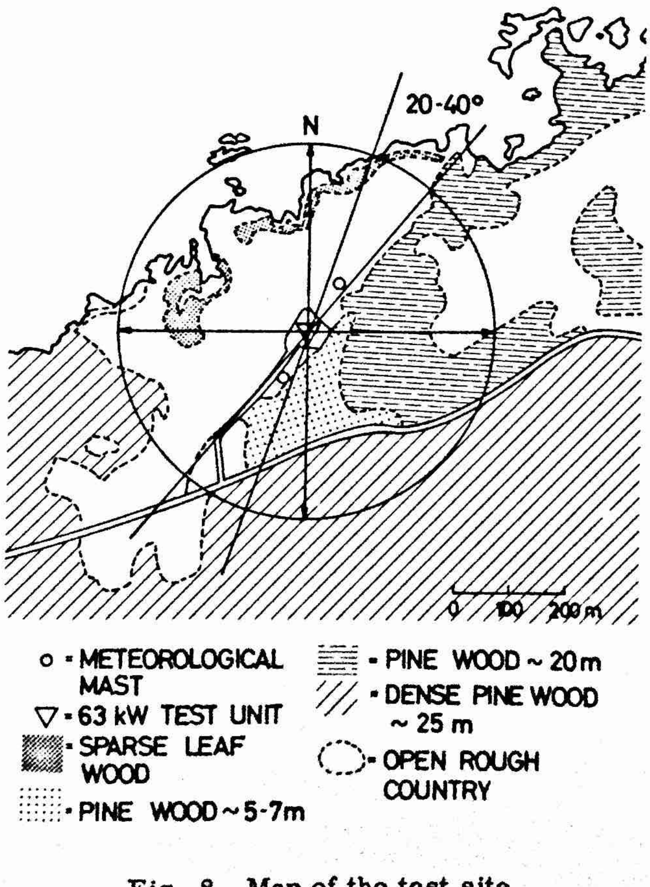

Fig. 8 Map of the test site

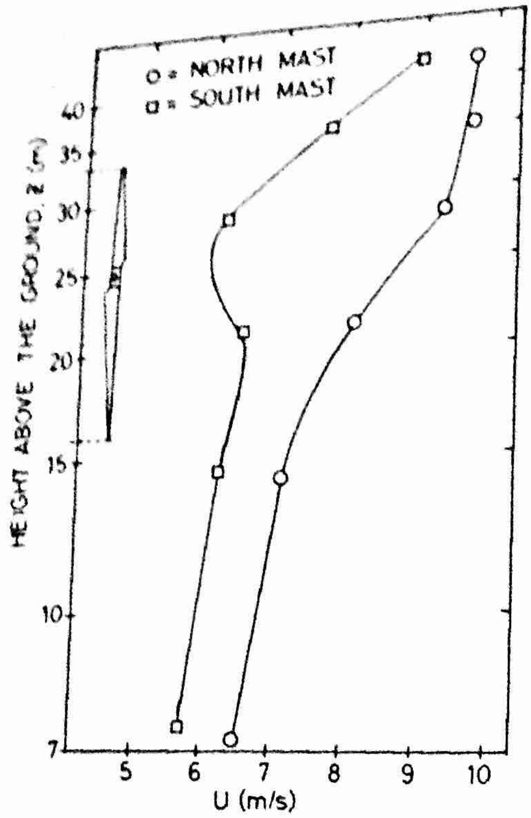

Fig. 9 One minute mean wind profiles from 7th. of October 1977 at 8.06 hour. The wind direction is 20^o-40^o during this minute and the mill is producing energy (24 kW). Logarithmic height scale

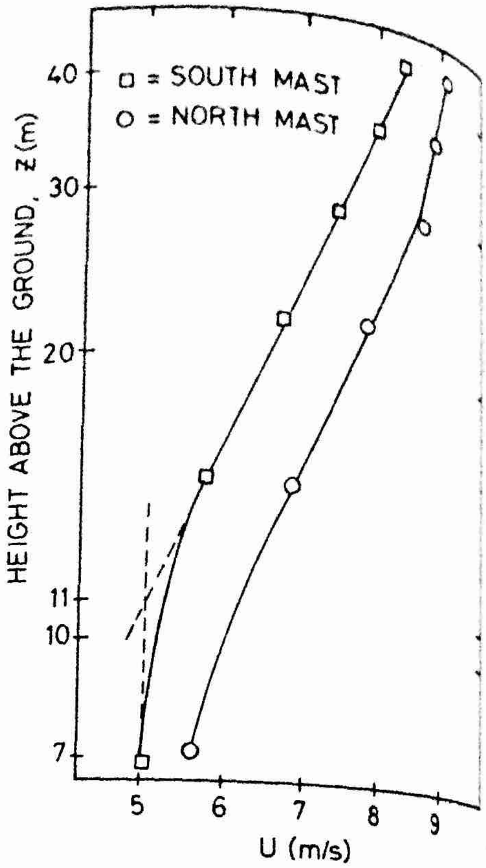

Fig. 10 Mean windprofiles October-November 1977 from the sector 20^o-40^o. Logarithmic height scale. Dotted lines are used for reconstructing profiles (see text)

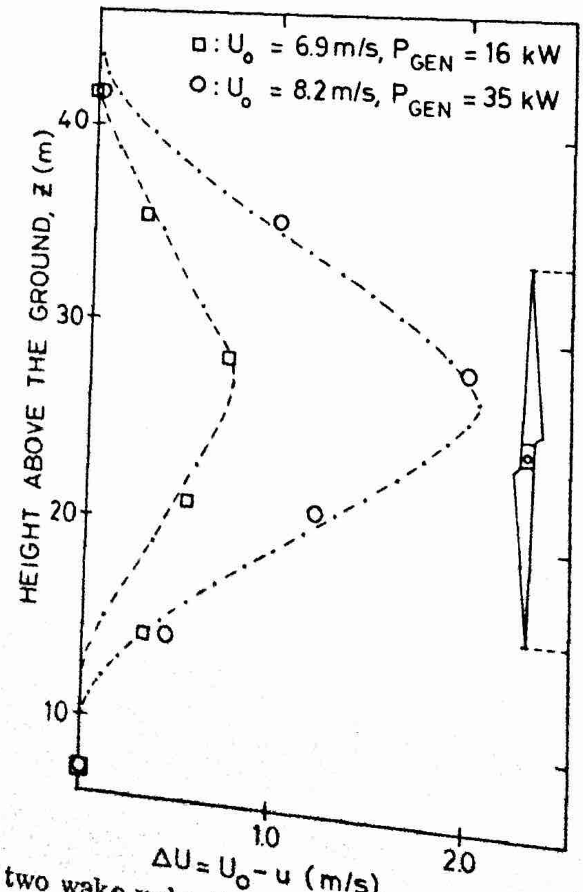

Fig. 11 Example of two wake velocity deficit profiles from field test (circles and squares) and predicted by Lissaman model (dotted lines). U_o is the oncoming wind speed at hubheight. P_{GEN} is the measured produced generator power. Linear height scale.